

# Resonance and frequency-locking phenomena in spatially extended phytoplankton-zooplankton system with additive noise and periodic forces

Quan-Xing Liu,<sup>1,\*</sup> Bai-Lian Li,<sup>2,†</sup> and Jin Zhen<sup>1,‡</sup>

<sup>1</sup>*Department of Mathematics, North University of China, Taiyuan, Shan'xi 030051, People's Republic of China*

<sup>2</sup>*Ecological Complexity and Modeling Laboratory, Department of Botany and Plant Sciences, University of California, Riverside, CA 92521-0124, USA*

(Dated: June 7, 2018)

It is shown that natural systems are undeniable subject to random fluctuations, arising from either environmental variability or internal effects. In this paper, we present a spatial version of phytoplankton-zooplankton model that includes some important factors such as external periodic forces, noise, and diffusion processes. The spatially extended phytoplankton-zooplankton system is from the original study by Scheffer [M Scheffer, Fish and nutrients interplay determines algal biomass: a minimal model, *Oikos* **62** (1991) 271-282]. Our results show that the spatially extended system exhibit a resonant patterns and frequency-locking phenomena. The system also shows that the noise and the external periodic forces play a constructive role in the Scheffer's model: first, the noise can enhance the oscillation of phytoplankton species' density and format a large clusters in the space when the noise intensity is within certain interval. Second, the external periodic forces can induce 4:1 and 1:1 frequency-locking and spatially homogeneous oscillation phenomena to appear. Finally, the resonant patterns are observed in the system when the spatial noises and external periodic forces are both turned on. Moreover, we found that the 4:1 frequency-locking transform into 1:1 frequency-locking when the noise intensity increased. In addition to elucidating our results outside the domain of Turing instability, we provide further analysis of Turing linear stability with the help of the numerical calculation by using the Maple software. Significantly, oscillations are enhanced in the system when the noise term presents. These results indicate that the oceanic plankton bloom may partly due to interplay between the stochastic factors and external forces instead of deterministic factors. These results also may help us to understand the effects arising from undeniable subject to random fluctuations in oceanic plankton bloom.

PACS numbers: 87.23.Cc, 05.40.-a, 82.40.Ck

## Contents

<b>I. Introduction</b>	1
<b>II. Model</b>	3
<b>III. Results</b>	4
A. Dynamics under the presence of noise only	4
B. Dynamics under the presence of the external forces only	5
C. Dynamics under both noise and external forces	7
<b>IV. Conclusion and Discussion</b>	7
<b>Acknowledgments</b>	8
<b>A. Stability analysis with the help of Maple</b>	9
<b>References</b>	10

## I. INTRODUCTION

Many mechanisms of the spatiotemporal variability of natural plankton populations are not known yet. Pronounced physical patterns, such as thermoclines, upwelling, fronts, and eddies, often set the frame for the biological process. While many parameters and variables can be learned from standard oceanographic measurements of temperature, salinity, nutrients, and biomass concentrations of phytoplankton and zooplankton, now new technologies such as remote sensing are being developed for observing the ecosystem. Measurements of the underwater light field are made with state-of-the-art instruments and used to calculate concentrations of phytoplankton biomass, such as chlorophyll, as well as other forms of organic matter. More recently, satellite remote sensing and detailed numerical simulations identify some spatial patterns including filaments, irregular patches, sharp gradients, and other complex structures involving a wide range of spatial scales and time scales by utilizing the species' concentration [1, 2, 3]. Figure 1 shows two pictures deriving from the field observation by the satellites remote sensing, where color gives us very useful information and ideas about the changes of chlorophyll concentrations in the two-dimensional spaces. The more pictures about the spatial patterns of the phytoplankton can be

\*Electronic address: liuqx315@sina.com

†Electronic address: bai-lian.li@ucr.edu

‡Corresponding author; Electronic address: jinzhn@263.net

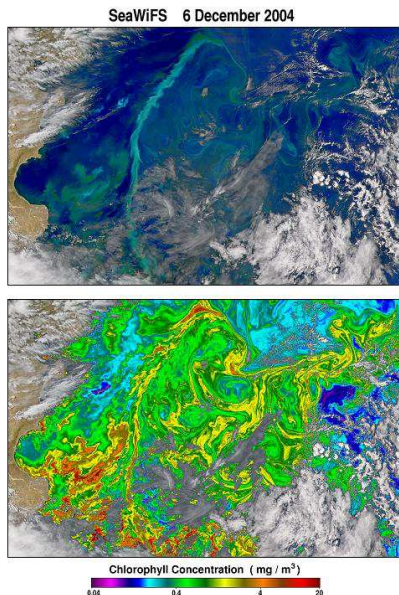


FIG. 1: (Color online) This satellite images are the field observation of the phytoplankton blooms in the Malvinas current region. The enhanced natural color images show actual differences in water color while the pseudocolor image shows chlorophyll concentration. The images are taken from <http://oceancolor.gsfc.nasa.gov>, with permission from Janet W. Campbell.

obtained from the web <http://oceancolor.gsfc.nasa.gov>, such as the stripelike, spotted-like, clockwise-rotating (or counterclockwise-rotating) spiral waves, spatial chaotic patterns, etc. Especially, In Ref. [1] from an observing system for monitoring the ecosystem is approached by posing five questions: How is the ecosystem changing? What are the forcing factors causing it to change? How does the ecosystem respond to natural and human forces? Can we predict future changes? And what are the consequences for stakeholders in our region?

Learning from historical records and from our field observations in Refs. [4, 5], one knows that the timing and magnitude of phytoplankton blooms vary significantly on interannual to longer timescales. For example, in some years, e.g., 2002, the spring bloom phytoplankton occurred in April, coinciding with vernal flowering on land, whereas in other years, e.g., 1999, the bloom occurred in February. Although there are only a handful of dynamics states that phytoplankton populations may exhibit stable equilibrium, deterministic extinction, stable population oscillations, and irregular fluctuations, there is a long list of factors that may interact to determine the community dynamics, e.g, competition, predation, parasitism, mutualism, age, stage and genetic structure, spatial structure of the habitat, climate, physical and chemical parameters. Thus, a key step in analyzing the community's dynamics is to untangle these mixtures of interacting factors and to identify their essential for the observed dynamics. Especially, from the experimental plankton

communities [6] [rotifer-algal] one knows that: first, the age structure of the predator populations is necessary to generate qualitatively correct predictions of population dynamics such as stability versus cycles. Second, the rapid evolution of population, including the alga and rotifers, is regarded as critical processes occurring on the same time scale in the ecological dynamics, and learned that microcosms may not just serve as a means to check model's assumptions, but that the results of microcosm studies can lead to novel insights into the function of biological communities. From Refs. [7, 8, 9], we know that the interannual variation in zooplankton and phytoplankton species might be the result of changes in climate, and the photosynthetic of the phytoplankton growth strongly depends on the intensity of the light. Hence, these period factors are regarded as the external periodic forces in the plankton systems. The variances of species evolving in time and space may be well understood.

Besides these periodic factors, there are many other stochastically factors causing phytoplankton-zooplankton blooms to transit extinction. For example, the effects arise from rivers' pollution on the phytoplankton-zooplankton ecosystem is one of the ways that humans affect the marine ecosystem. Large rivers are major mechanisms for nutrient delivery to the ocean. Hence, the quality of river water affects freshwater ecosystems and oceanic food webs. Away from this, the long term climatic variation also shows the stochastic factor for the ecological system [see [10] for giving a review about this points]. In the phytoplankton-zooplankton systems, the random fluctuations also are undeniably arising from either environmental variability or internal species. To quantify the relationship between fluctuations and species' concentration with spatial degrees of freedom, the consideration of these fluctuations supposes to deal with noisy quantities whose variance might at times be a sizable fraction of their mean levels. For example, the birth and death processes of individuals are intrinsically fluctuations [11], which become especially pronounced when the amount of individuals is small. The interaction between the oceanic zooplankton and fish, which are far from being uniformly distributed, also introduce randomness [12]. In addition, these processes can be regarded as parameter fluctuates irregularly with spaces and time. For example, phytoplankton production is effected by iron concentration, which can be elevated in surface water after rain [13]. These unavoidable fluctuations can also interact with the system's nonlinearities to render counterintuitive behavior, in which an increase in the noise level produces a more regular behavior [14]. Now, it is natural to ask what are spatiotemporal behaviors of the spatially extended plankton system if these external periodic forces and the irregular fluctuation factors work on. Especially, can the periodic oscillation retain to appear? In order to understand the stochastically force, we give the short introduction of the noise application in the physics and biology.

Recently, research interest has shifted to the effects

of noise in spatially extended system [14, 15]. Well-known examples in zero-dimensional (ODE) systems are noise-induced transition [16], stochastic resonance [17, 18, 19], enhanced spatial synchronization [20], and noise-sustained oscillations [21, 22, 23] [the reader can read an overview written by F Sagués in Ref. [14]]. More recently, effects of noise in spatially distributed systems, including noise-induced pattern formation [14, 24, 25], noise-induced fronts [26, 27], etc, have been extended study by many communities. In these and other noise-related phenomena, multiplicative noise, which couples to the system state plays a very special role. However, prominent effect has been also found for additive noise. Such influence has been observed in noise-induced pattern formation [18, 25, 28, 29, 30]. A recent report [31] demonstrated that additive noise which globally alternates between with two different monostable excitable dynamics yields pattern formation. Meanwhile, in recent years several theoretical investigations have been done on noise-induced effects in population dynamics, see [32, 33, 34, 35, 36, 37, 38, 39]. Noise, such as that from the natural variability, are inevitably presented in these type of systems, but its effects have not yet been addressed completely. In this paper, we report resonant patterns and frequency locked oscillations induced by additive noise and external forces in phytoplankton-zooplankton systems, and take into account the interplay among noise, external forces, and diffusion processes. In

the following, we first give the spatially extended model and method we used, and then the describe our results.

## II. MODEL

From the recent perspective of Pascual [40], the physical environments play an important role in the biota. If the climate sharply changes, the population abundance will change. Especially, the spatiotemporal dynamics of global population abundance, such as aggregated over the whole space, can be approximated by mean-field-type equations in which the functional forms specifying the growth rates and interactions have been modified as power functions. And, the effect of interactions on local (or individual scales) can be represented implicitly by the changed form of the functions to describe interactions on global scales. We want to focus on the effects of a periodic varying and the stochastic fluctuation factors to the spatially extended phytoplankton and zooplankton model. Following Scheffer's minimal approach [41] and the previous analysis [42, 43, 44, 45], we study a two-variable phytoplankton and zooplankton spatial model involving time-periodic forces and the fluctuation term to describe the influence of spatial noise on pattern formation. The spatially extended model is written as

$$\frac{\partial p}{\partial t} = rp(1-p) - \frac{ap}{1+bp}h + A \sin(\omega t) + d_p \nabla^2 p, \quad (1a)$$

$$\frac{\partial h}{\partial t} = \frac{ap}{1+bp}h - mh - f \frac{nh^2}{n^2+h^2} + A \sin(\omega t) + \eta(\mathbf{r}, t) + d_h \nabla^2 h, \quad (1b)$$

where the parameters  $r$ ,  $a$ ,  $b$ ,  $m$ ,  $n$ ,  $d_p$ ,  $d_h$ , and  $f$  refer to the previous works [42, 43] on the dimensionless model (1) absence of periodic force and noise term. Here  $p(x, y, t)$  and  $h(x, y, t)$  are scalar fields representing the concentrations of phytoplankton species and zooplankton species in the two-dimensional space. It must also be kept mind that the individuals of the population have not been at the same point in space at previous times, so they are a function of time. The periodic force is assumed to be sinusoidal with amplitude  $A$  and frequency  $\omega$ . The periodic force is considered as additive version for reason that toxins produced by different phytoplankton species has a significant role in shaping the dynamical behavior of marine plankton ecosystems [46]. The zooplankton population tries to avoid the areas where the concentration of phytoplankton is very large. The reason may be either dense concentration or the effect

of toxic substance released by phytoplankton, of course including the others factor as introduced in previous section, such as human action, nature sharp changing-red tides and localized outbreaks and occur in coastal water and fronts [47]. Buskey and Stockwell [48] have shown in their field study that macro- and meso-zooplankton populations are reduced during the blooms of Chryso-phyte (*Aureococcus anophagefferens*). These factors are not directly correlated with species internal parameters, so that the  $A \sin(\omega t)$  be added in the equation instead of  $Ap(1-p) \sin(\omega t)$ . Such consideration is meaningful in the biology systems (see Ref. [43, 49]). In Eq. (1), the stochastic factors are taken into account as the term,  $\eta(\mathbf{r}, t)$ . Of course, due to the coupling, the noise in Eq. (1b) will have its influence on Eq. (1a) as well. The noise term  $\eta(\mathbf{r}, t)$  is introduced additively in space and time, which is the Ornstein-Uhlenbeck process that obeys

the following stochastic partial differential equation [50]:

$$\frac{\partial \eta(\mathbf{r}, t)}{\partial t} = -\frac{1}{\tau} \eta(\mathbf{r}, t) + \frac{1}{\tau} \xi(\mathbf{r}, t), \quad (2)$$

where  $\xi(\mathbf{r}, t)$  is a Gaussian white noise with zero mean and correlation,

$$\langle \xi(\mathbf{r}, t) \xi(\mathbf{r}', t') \rangle = 2\varepsilon \delta(\mathbf{r} - \mathbf{r}') \delta(t - t'). \quad (3)$$

The colored noise  $\eta(\mathbf{r}, t)$ , which is temporally correlated and white in space, satisfies

$$\langle \eta(\mathbf{r}, t) \eta(\mathbf{r}', t') \rangle = \frac{\varepsilon}{\tau} \exp\left(-\frac{|t - t'|}{\tau}\right) \delta(\mathbf{r} - \mathbf{r}'), \quad (4)$$

where  $\tau$  controls the temporal correlation, and  $\varepsilon$  measures the noise intensity.

In this work, we rely on numerical simulations of the model of Eqs. (1) and (2). We here consider spatiotemporal evolution of this system with space white noise and colored noise evolving in time when the system lies within the regime of self-sustained Hopf oscillation. Note that the explicit form of the noise term represents only on the fluctuating recruitment rate (or death rate) has been studied by Malchow et al [11], in which the parameter  $m$  only is regarded as noise form, i.e.,  $m = m_0 + \xi(t)$ ,  $\xi(t)$  denotes Gaussian white noise. For the absence of the external periodic forces and colored noise, Hopf instability occurs and spatially homogeneous oscillation comes up when the parameter  $f$  less than the critical value  $f_H = 0.3398$  [see Appendix A] whose value depends on the other parameters. Moreover, from previous analysis and numerical simulations [51, 52] show that spiral waves structure exists in the two-dimensional space and the spatiotemporal chaos will emerge through its far-field breakup when the parameter  $f$  within the mixed domain of the Hopf-Turing instability, but the parameters are outside the Turing instability domain in present paper [see Appendix A for a simple analysis]. In fact, from recent perspective that the 2:1 resonance phenomena on the spiral wave may will appear when the system undergoes saddle-node or Hopf bifurcation [53]. In other words, the temporal period of the bifurcation patterns is twice the period of the primary spiral, i.e., the Hopf frequency  $\omega_H$  needs to be in a 2:1 resonance with the rotation frequency of the spiral wave. However, here we show that the system also exhibits spatiotemporal chaos patterns and the 4:1 and 1:1 resonances with the period of the external forces when fluctuations and periodic forces are considered. Except when it explicitly is pointed out, we take parameters  $r = 5$ ,  $a = 5$ ,  $b = 5$ ,  $m = 0.6$ ,  $n = 0.4$ ,  $f = 0.3$ ,  $d_p = 0.05$ , and  $d_h = 0.5$  throughout this paper. These parameters estimate by Medvinsky et al [42, 43, 44]. From these References, we know that these parameters are meaningful from the ecological point of view. The noise intensity  $\varepsilon$  and correlation time  $\tau$  are adjusted as control parameters.

### III. RESULTS

Extensive testing was performed through numerical simulations to the described model (1) and the results are shown this section. In simulation, zero-flux boundary conditions are used and time step  $\Delta t = 0.05$  time unit. The space step  $\Delta x = \Delta y = 1$  length unit and the grid sizes in the evolutionary simulations are  $N \times N$  ( $N = 200$ ). The Fourier transform method is used for the deterministic part in Eq. (1). On the discrete square lattices, the stochastic partial differential Eq. (2) is integrated numerically by applying the Euler method. Several different discrete methods (simple Euler, Runge-Kutta, and Fourier transform) was checked, and the results indicate that Fourier transform accurately approximates solutions of Eq. (1). On the other hand, the Fourier method offers the speed advantage over other numerical methods. We find that on the PC computer the Fourier method runs about 3-4 times faster than the Euler integration using the same time step and space step. Code is implemented in Matlab 7.3 and the *fft2*, *fftshift*, *ifft2*, and *ifftshift* functions were used for the main numerical integration.

Although the noisy fluctuations may sometimes causing the variable ( $p$  and  $h$ ) to be less than zero, it will lead to the diffusion-reaction system with cutoff effect at low densities when the species extinction is taken into account explicitly [54]. According to the spatially extended model (1), at each position in space, whenever the population densities fall below certain prescribed value  $\varepsilon$  they are set to zero or sufficient small positive constant [54, 55]. From the biological point of view, in this paper we set that they equal to 0.0001 when the variables change to negative. Note that we are not much concerned here with the ‘‘exact’’ value of  $\varepsilon$ , for the reason that an attempt to estimate the ‘‘exact’’ value would hardly make any ecological sense in terms of very schematic model (1). To compare with the numerical results under the different cases, we used the same initial conditions that are randomly perturbed (the perturbations are space-independent) by homogenous equilibrium  $(p^*, h^*) = (0.3944, 1.7998)$ , except when they are explicitly pointed out.

#### A. Dynamics under the presence of noise only

In the ecological systems, noise-sustained and noise-induced spatial pattern formations have been discussed in recent years [33, 34, 35, 36, 37, 38, 39]. For the convenience of discussion about the resonant pattern formation induced by additive noise and the external forces, here we first present a brief description about the affection arising from the fluctuations in the system (1). From our results show that the sole noise also plays a constructive role in the model (1) by maintaining (or eliminate) the large spatial clusters [cf. Fig. 3, 4 and partly *movie-1*, *movie-2*, *movie-3*] and enhancing the aperiodic oscillation [see Fig. 5]. Some typical snapshots of the spatial patterns at

$t = 300$  presented in Fig. 2, and Fig. 3, 4, where before and after the noise is added, respectively [see caption of Figures]. The ratio's distribution of two species is a key measurement in the ecological field. To characterize this measurement in the system (1), we introduce the parameter,  $\theta$  (the  $\theta \in [-2\pi, 2\pi]$ ) and define as following:

$$\theta = \arg((p_{s,k} - p^*) + i(h_{s,k} - h^*)), \quad (5)$$

where  $s, k = 1, 2, \dots, N$ .  $\theta$  indicates the relation between the two variables of the system, called the phase angle. Note that it also depicts the variance of the amplitude relevant the two species in the space, for the reason that its variables are the difference around the stable points,  $p^*$  and  $h^*$ . Similarly, the following parameter,  $\mathcal{L}$ , depicts the average amplitude for the system in the space. However, we find that it is equivalent to the mean value of the variables in this system [cf. Fig. 2,7,8, and Fig. 5], so we only use it in this section.

$$\mathcal{L} = \ln\left(\frac{\sqrt{\sum(p_{s,k} - p^*)^2}}{N}\right), \quad (6)$$

where  $s, k = 1, 2, \dots, N$ . The spatiotemporal chaotic spiral patterns appears when the noises are free [see Fig.2], and the large clusters can be recognized in the space. The  $\mathcal{L}$  or  $\langle p \rangle$  (the  $\langle p \rangle$  denotes the spatial average of  $p$  rather than the time average) oscillates with small fluctuations (quasi-period) [56], as shown in Fig.2(d) (and Fig. 5), in which the abscissa is time and the ordinate is variable,  $\mathcal{L}$ . The behavior of the system undergoes drastic changes when the noises are turned on (cf. Fig. 2, 3, and 4). First, the large spatiotemporal chaotic clusters die out gradually with the increasing of noise intensity; second, the oscillations of  $\mathcal{L}$  become more obvious when noise intensity is within a certain regions, but it stays at a fixed value again if the noise intensity is further increasing. In sum, compared with Fig. 2, 3, and 4, it should be noted that the noise plays a constructive role in the relation between phytoplankton and zooplankton in the space.

### B. Dynamics under the presence of the external forces only

From the previous analysis [8], it is known that the plankton system (1) has a very complex dynamical behaviors such as the scenario of bifurcations and chaos when the system was not considered the spatial degree of free. However, we here consider the case that the parameter values are within the Hopf oscillation interval and the spatial degree of free was taken into account.

The parameter values under we take in previous Section II, and also the system is noise free in this subsection, thus the spatially homogeneous oscillation does not respond to the external periodic force if the amplitude  $A$  is below a threshold  $A_c$ , whose value depends on the external period  $T_{in} = \frac{2\pi}{\omega}$ . Above the threshold, the system (1)

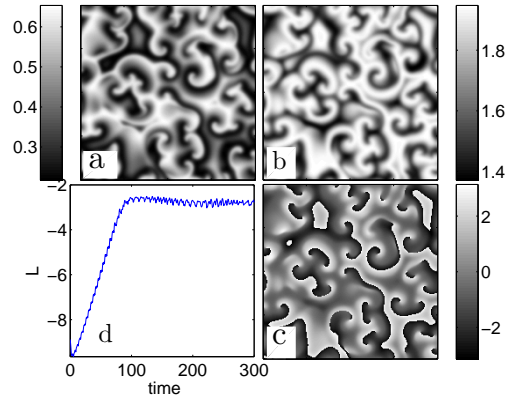


FIG. 2: A typical grey-scaled snapshots of spatiotemporal chaotic patterns at  $t = 300$ , when the system (1) evolves in time without noise term. (a) and (b) the spatial patterns of  $p$  and  $h$ , respectively; (c) the phase angle,  $\theta$  (see the definition in text); (d) the amplitude,  $\mathcal{L}$  evolves in time. [see the *Movie-1*, and additional movies format available from Ref. [57]]

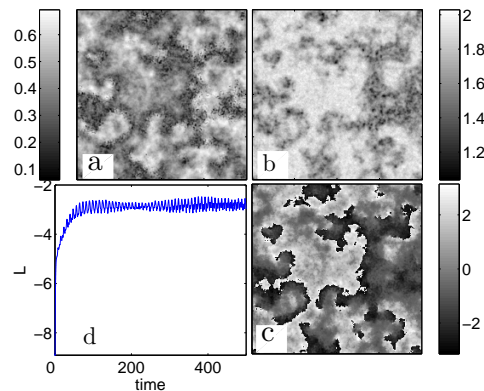


FIG. 3: A typical grey-scaled snapshots of spatiotemporal chaotic patterns at  $t = 300$ , when the system (1) evolves in time with noise term. The meanings of the images are correspondent to the Fig. 2, with the values of the parameters are  $\tau = 1$  and  $\varepsilon = 0.001$ . [see the *Movie-2*, and additional movies format available from Ref. [57]]

produces oscillations about period  $T_{out}$  with respect to external period  $T_{in}$ , this phenomena are called frequency locking or resonant response, i.e., when the system produces one spike within each of the  $M$  ( $M = 1, 2, 3, \dots$ ) periods of the external force, that is,  $M : 1$  resonant response. In present paper, the output period  $T_{out}$  is defined as follows:  $T_i$  is the time interval between the  $i$ th spike and the  $i + 1$ th spike.  $q$  spikes are taken into account and the average value of them is  $T_{out}$ , where

$$T_{out} = \frac{\sum_{i=1}^q T_i}{q-1} \quad [58].$$

Two types of frequency locking phenomena are observed in the spatially extended model (1). They are

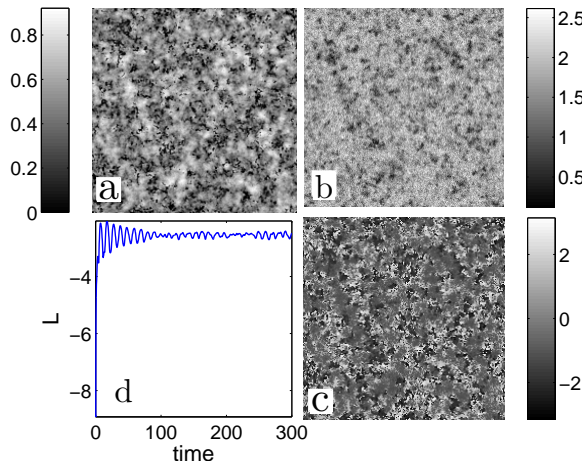


FIG. 4: A typical grey-scaled snapshots of spatiotemporal chaotic patterns at  $t = 300$ . Same situation as the Fig. 3 but  $\varepsilon = 0.05$ . [see the *Movie-3*, and additional movies format available from Ref. [57]]

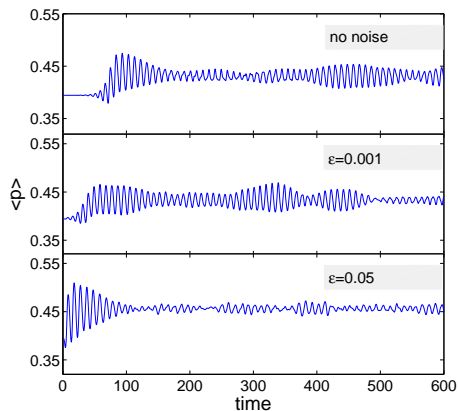


FIG. 5: Directly compare with the mean values of variable  $p$  without and with noise term. Same situation as the Fig. 2-4.

4 : 1 and 1 : 1 frequency locking. In Fig. 6(a) and (b), we have plotted the temporal evolution of the variable  $p$  when the amplitude  $A$  is above the threshold, where the 4 : 1 and 1 : 1 frequency lockings take place, respectively. In these cases, the spatially homogeneous oscillation patterns depend on the initial conditions, and two-phase patterns with a phase shift and separated by stationary Ising front [In particular, for the initial conditions coming from the Ref. [43] that is  $p(x, y, 0) = p^*$ , and  $h(x, y, 0) = h^* + \epsilon x + \delta$ , here  $\epsilon$  and  $\delta$  are parameters.], or alternative homogeneous oscillations come out [see Fig. 6(c)]. From the random initial conditions prepared by randomly perturbing around the homogeneous steady state  $(p^*, h^*)$ , we obtain 4 : 1 resonant homogeneous oscillations, as an example shown in Fig. 6(c),

which plots the space-time figure for the homogeneous patterns to compare with the external force, and illustrates that the patterns are well 4 : 1 frequency locking. Moreover, the 4 : 1 frequency locking was demonstrated with a power spectrum as shown in Fig. 10, i.e.,  $T_{out} : T_{in} = \frac{1}{\omega'} : \frac{2\pi}{\omega} = 4 : 1$ . Note that the green lines in Fig. 6 only denote the exact temporal period of the external forces rather than its values to comparing.

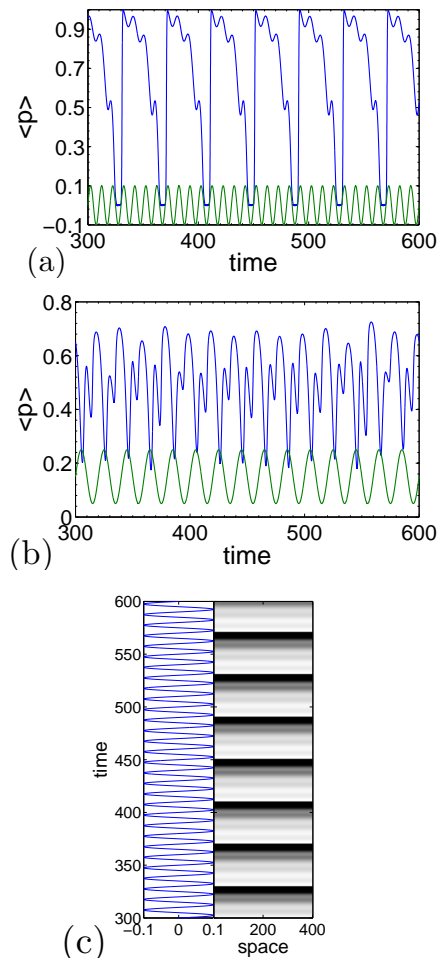


FIG. 6: (color) Sequences of the mean concentration  $\langle p \rangle$ , the noise free. (a) The 4 : 1 frequency locking oscillation with the values of the parameters are  $A = 0.1$  and  $\omega = 2\pi \times 10^{-1}$ . (b) The 1 : 1 frequency locking oscillation with the values of the parameters are  $A = 0.1$ , but  $\omega = \pi \times 10^{-1}$ . (c) Space-time diagram (right panel) displays the time evolution of the patterns in the one-dimensional space. For comparison, the curve at the left panel shows the periodic external force. In panel (c), the left and right window share the same ordinate which is time. Note that the green lines only denote the exact temporal period of the external forces rather than its values to comparing.

### C. Dynamics under both noise and external forces

Now, we turn on the additive noise and periodic forces in the system (1). To check their effects on the system (1) within the 4 : 1 frequency locking regimes, we adjust the noise strength and correlation time. At first series of simulations, we adopt  $\tau = 1.0$ , and adjust the noise intensity,  $\varepsilon$ . Considering the influences of noise and spatial distribution on the system, we performed simulation starting at  $\varepsilon = 0.001$ , and then  $\varepsilon$  is increased in small steps  $\Delta\varepsilon = 0.001$  until the noise intensity is enough large values. The noise drastically changes the previous scenarios in the system including the spatial patterns and frequency locking when the noise intensity is strong enough [see Fig. 7]. First, the spatial patterns with homogeneous oscillation are replaced by the spatial heterogeneous oscillations. This means that the distribution of the species may appear spatial patterns and its bloom is periodic in the space when some fluctuations work on the system [see Fig. 7(a)]. Second, the frequency locking (4 : 1) shifts into the other type frequency locking (1 : 1) [see Fig. 7(b)].

From our numerical results [cf. Fig. 7], one could conclude that homogeneous oscillations depends on the noise intensity. The oscillations are only slightly perturbed, or not affected when the noise intensity  $\varepsilon$  is small. As  $\varepsilon$  is increased, the homogeneous oscillating patters lose its stability and associate with the frequency locking changed. Figure 7(a) (middle column) shows that oscillating two-phase pattern with local spotted patterns will appear at  $\varepsilon = 0.001$ . When the noise intensity further is increased, the spotted patterns show aggregation behaviour, and become a large clusters in the space. Figure 7(a) (right-hand column) shows a clear spatial oscillation patterns with a large clusters will appear at  $\varepsilon = 0.050$ . In Fig. 7(b) we have plotted the temporal evolution of the variable  $\langle p \rangle$  when the noise intensity is taken different values. It is interesting to realize that the resonant patterns and the frequency locking do not alter by increasing the noise intensity within the large interval [e.g. 0.0005 to 0.001; 0.05 to 0.10]. The variable  $\langle h \rangle$  also exhibits the similar characteristics in model.

In order to elucidate the evolutionary processes of the spatial structure, we have depicted typical spatiotemporal patterns of the system (1) within one period  $T_{out}$ , as shown in Fig. 8 and the *movie-6*. The other periods also exhibit the similar characteristics.

The previous Figs. 6 and 7 exhibit an aspect about the frequency locking and resonant pattern which have received considerable attention in the recent years, namely, the response of the system to a periodic forces may be enhanced by the presence of noise [14, 18, 23, 30, 59, 60].

The role of temporal correlation  $\tau$  of the colored noise is the other significant except it intensity in inducing and controlling the spatial patterns formation and transition of the resonant patterns. Now, it is natural to ask what is the effect consequence of the temporal correlation of the colored noise. Especially, the phase diagram of the

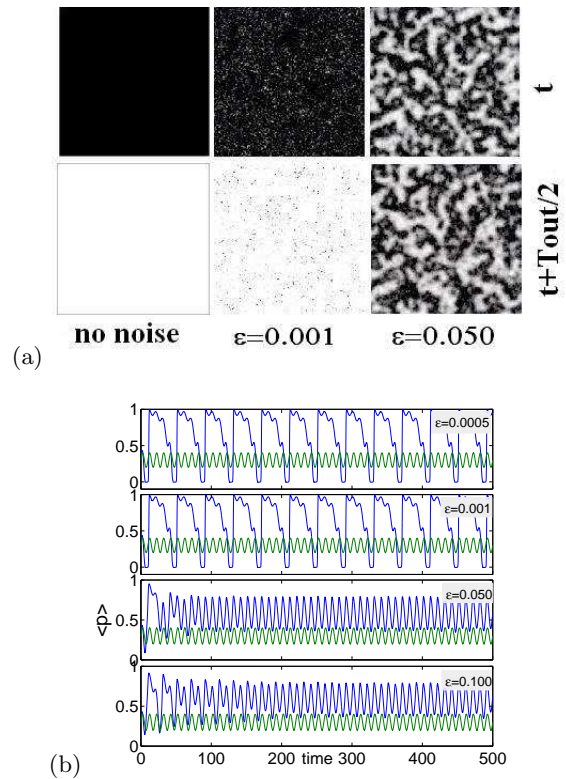


FIG. 7: Spatial frequency locking patterns and the time series of the mean value  $\langle p \rangle$  of the concentration  $p(x, y)$  with respect to different noise intensities  $\varepsilon$ . (a) Grey-scaled snapshots of spatial frequency locking patterns with different noise intensities  $\varepsilon$ , where the noise intensity is 0.001 and 0.05 for middle column and right-hand column. (b) The change of the frequency locking with respect to the different noise intensities. Same situation as the Fig. 6(a) but  $\varepsilon$ . [see the *Movie-4*, *Movie-5* for Fig. 7(a), and additional movies format available from Ref. [57]]

$\varepsilon - \tau$  parameter space. In order to well understand the phase transition by the influence of temporal correlation  $\tau$ , we performed a series of simulations, fixing the  $\tau$  and scanning the noise intensity,  $\varepsilon$ , when the frequency locking evidently changes in the long term [here we run the time up to 5000] and recorded the data. Figure 9 summarizes the results from the numerical simulations, in which the region A and B are corresponding to the 1:1 frequency locking and 4:1 frequency locking respectively. Figure 9 depicts the transition point of frequency locking shifts toward higher values of the noise intensity as the correlation time is increased, that is,  $\tau$  softens the effect of the noise.

## IV. CONCLUSION AND DISCUSSION

It is known that, an external periodic forces applied to a nonlinear pendulum can cause the pendulum to become entrained at a frequency which is rationally related to the applied frequency, a phenomenon known as

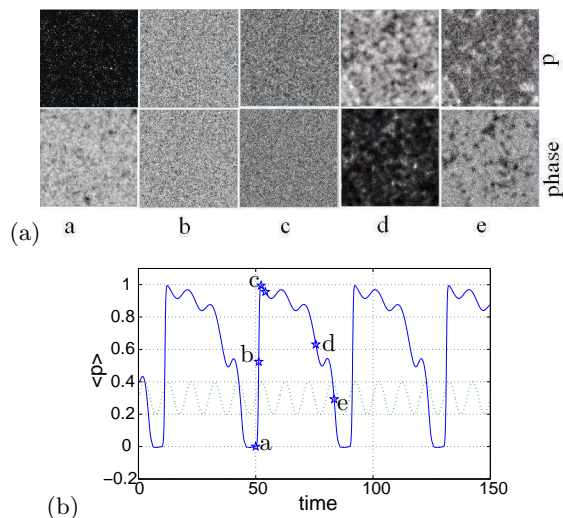


FIG. 8: Typical spatial pattern formation to the forces-noise system (1) within the 4:1 frequency locking region as in case Fig. 7(b) [ $\varepsilon = 0.005$ ]. (a) Grey-scaled snapshots of spatial patterns of the variable  $p$  and the phase angle,  $\theta$ . [the time from the left to right]. (b) shows the time series of the mean concentration  $p$  corresponding to the snapshots in (a). [see the *Movie-6* for Fig. 8(a), and additional movies format available from Ref. [57]. Note that the movie is 25 frames per second].

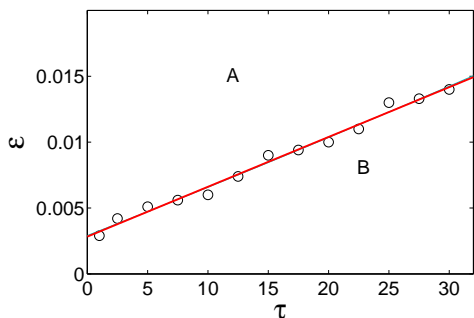


FIG. 9: Phase diagram in  $\varepsilon$ - $\tau$  parameter space, with  $A = 0.1$  and  $\omega = 2\pi \times 10^{-1}$ . There are two states: 4:1 region (B) and 1:1 region (A). The solid lines is a least-square fit of circles data.

the frequency-locking [61]. A recent theoretical analysis shows that an array of coupled nonlinear oscillators can exhibit spatial reorganization when they subjected to external periodic forces [62]. In this paper, we present a spatial version of phytoplankton-zooplankton model that includes some important factors such as external periodic forces, random fluctuations, and diffusion processes. The modified system based on the original model by Scheffer [41, 42], but here it can exhibit frequency-locking phenomena and resonant patterns. Our results show that the noise and the external periodic forces play a constructive role in the Scheffer's model: first, the noise can enhance the oscillation of the species' density and format a large clusters in the space. Second, the external peri-

odic forces can induce 4:1 and 1:1 frequency-locking and spatially homogeneous oscillation to appear. Third, the resonant patterns are observed in the system when the spatial noise and external periodic forces are turned on, moreover the frequency-lockings transit when the noise intensity increased. These result from outside the domain of Turing instability. In the Appendix A, we further provide a simple Turing linear stability analysis with the help of the numerical calculation by using the Maple software.

It is worth emphasizing that the frequency lockings and resonant patterns only appear when noise and the external forces present in the model (1). We here consider the cases when the unforced system lies outside the Turing instability [see Appendix A for details]. The typical power spectra  $P(\omega')$  related to the density of the phytoplankton for the oscillations within 4:1 frequency locking is analysis, as shown in Fig. 10. The power spectra related to the density of zooplankton [not shown here] is similar. The presence of a prominent and well defined peak in the power spectrum of Fig. 10 at a nonzero frequency characterize oscillating behavior. From Fig. 10, one could see that the oscillation behavior relates to the external periodic forces and the natural frequency,  $\omega_H$  [see the Appendix A] of the system. Significantly, oscillations are enhanced in the system when the single noise term presents. These results indicate that the oceanic plankton bloom may partly due to the interplay between external forces and stochastic factors instead of deterministic factors. Our results also may help us to understand the effects arising from undeniable subject to random fluctuations in oceanic plankton bloom.

In this paper, we study the effects of noise and external forces on spatially extended phytoplankton-zooplankton system in static media (no prominent the advection term). However, in the oceanic ecological systems the biological processes among the species are in a fluid environment, such as turbulent flows or chaotic advection. Recently, a few authors consider the mixing of the flow and diffusion processes using a well-known standard model of chaotic advection [3, 23, 63, 64, 65, 66, 67, 68] in the excitable media, especially, Reigada et al [69] found that plankton blooms also can be induced by turbulent flows. So, a further study in our work will analyze the effects arising from the mixing of the advection, diffusion, the external forces and noise. It is also interesting to apply the problem of oceanic plankton bloom and the spatial structure observed by the field as a introduction in Section I.

### Acknowledgments

We thank Professor Janet W. Campbell, the Center of Excellence for Coastal Ocean Observation and Analysis (COOA), for providing and permitting us using the satellite images, Fen-Ni Si, China Academy of Engineering Physics, for enlightening discussion about the colored

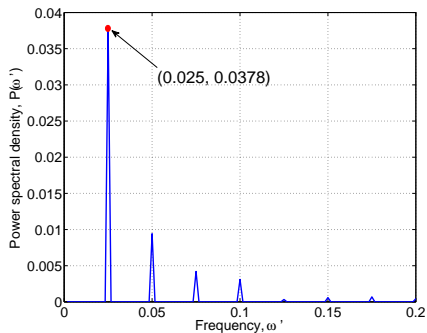


FIG. 10: Corresponding the power spectrum for the density of variable  $p$  as a function of its frequency with the parameters values  $\omega = 2\pi \times 10^{-1}$  and  $\varepsilon = 0.001$  [the same as Fig. 6(a)]. Note that the period was normalized to units so that  $T_{out} = 1/\omega'$ .

noise, and Professor Weiming Wang, School of Mathematics and Information Science, Wenzhou University, for reading the original manuscript. The authors thank Professor R. Reigada from the University of Barcelona for pointing out Ref. [69]. This work was supported by the National Natural Science Foundation of China under Grant No. 10471040, the Natural Science Foundation of Shan'xi Province Grant No. 2006011009, and the Youth Science Foundation of Shan'xi Province 2007021006.

#### APPENDIX A: STABILITY ANALYSIS WITH THE HELP OF MAPLE

This appendix is devoted to the numerical analysis of unforced system (A1).

$$\frac{dp}{dt} = rp(1-p) - \frac{ap}{1+bp}h, \quad (\text{A1a})$$

$$\frac{dh}{dt} = \frac{ap}{1+bp}h - mh - f\frac{nh^2}{n^2+h^2}, \quad (\text{A1b})$$

Setting the left-hand sides of system (A1) to zero, we obtain

$$g_1(p, h) = rp(1-p) - \frac{ap}{1+bp}h, \quad (\text{A2})$$

$$g_2(p, h) = \frac{ap}{1+bp}h - mh - f\frac{nh^2}{n^2+h^2}. \quad (\text{A3})$$

The Eqs. (A2) and (A3) exist a unique interior equilibrium  $(p^*, h^*)$ , when parameter  $f$  less than 0.445.

Now we consider the stability of this positive equilibrium. The Jacobian matrix at the positive equilibrium  $(p^*, h^*)$  is

$$J = \begin{pmatrix} \left[ \frac{\partial g_1}{\partial p} \right]_{(p^*, h^*)} & \left[ \frac{\partial g_1}{\partial h} \right]_{(p^*, h^*)} \\ \left[ \frac{\partial g_2}{\partial p} \right]_{(p^*, h^*)} & \left[ \frac{\partial g_2}{\partial h} \right]_{(p^*, h^*)} \end{pmatrix}. \quad (\text{A4})$$

TABLE I: The eigenvalues of the Jacobian matrix (A4)

$f$	0.30	0.3397	0.3398	0.3399
$\lambda_{1,2}$	$.0473 \pm .8221i$	$.0001 \pm .8040i$	$.0000 \pm .8039i$	$-.0001 \pm .8039i$

Its eigenvalues,  $\lambda_{1,2}$ , were listed in the Table I with the different parameter values  $f$ . The first type of instability is associated with a Hopf bifurcation in the spatially uniform system. This instability will appear at the threshold  $f_H$  and oscillate homogeneously with the natural frequency  $\omega_H = \text{Im}(\lambda_{1,2})$ . From Table I, one could see that the natural frequency equals to 0.8221 if  $f = 0.30$ .

Now we consider the spatial inhomogeneous perturbation by using the techniques of Koch and Meinhardt [70].

$$\delta p = \delta p_0 \exp(\lambda' t + i\mathbf{k}\mathbf{r}), \delta h = \delta h_0 \exp(\lambda' t + i\mathbf{k}\mathbf{r}), \quad (\text{A5})$$

with wave number vector  $\mathbf{k} = (k_x, k_y)$ ,  $|\delta p_0|, |\delta h_0| \ll 1$  and imaginary unit  $i^2 = -1$ . Due to the zero-flux boundary conditions,  $k_x$  and  $k_y$  take only discrete values

$$k_x^n = k_y^n = n\pi/L, n = 0, 1, 2 \dots, \quad (\text{A6})$$

where  $L$  is the size of the space. Each  $k_x^n$  is associated with a “frequency”  $\omega_n$ , which can be a complex number. The functions  $\omega_n(\mathbf{k}^n)$  are found by substituting expression (A5) into following equation

$$\frac{\partial p}{\partial t} = rp(1-p) - \frac{ap}{1+bp}h + d_p \nabla^2 p, \quad (\text{A7a})$$

$$\frac{\partial h}{\partial t} = \frac{ap}{1+bp}h - mh - f\frac{nh^2}{n^2+h^2} + d_h \nabla^2 h. \quad (\text{A7b})$$

Retaining terms up to first order in  $\delta p$  and  $\delta h$ , we get linearized equation:

$$J' \begin{pmatrix} \delta p \\ \delta h \end{pmatrix} = 0, \quad (\text{A8})$$

with

$$J' = \begin{pmatrix} \left[ \frac{\partial g_1}{\partial p} \right]_{(p^*, h^*)} - d_p(\mathbf{k}^n)^2 - \lambda' & \left[ \frac{\partial g_1}{\partial h} \right]_{(p^*, h^*)} \\ \left[ \frac{\partial g_2}{\partial p} \right]_{(p^*, h^*)} & \left[ \frac{\partial g_2}{\partial h} \right]_{(p^*, h^*)} - d_h(\mathbf{k}^n)^2 - \lambda' \end{pmatrix}. \quad (\text{A9})$$

TABLE II: The eigenvalues of the Jacobian matrix (A9)

$f$	0.30	0.3124	0.3125
$\lambda'_{1,2}$	$-0.0704 \pm 0.8177i$	$-0.0003 \pm 0.8174i$	$0.0003 \pm 0.8174i$
$\mathbf{k}_c^n$	0.6539	0.3480	0.3444

The perturbation amplitudes  $\delta p_0$  and  $\delta h_0$  can be different from zero if and only if the  $\det J' = 0$ .

Turing instability is expected to occur for finite  $\mathbf{k}^n > 0$ , and at least one of the real parts becoming greater than zero. If  $f$  is taken as a control parameter, the critical point is reached if the determinant  $J'$  has a pure imagi-

nary eigenvalue, i.e.,  $f = f_T$ ,  $\text{Re}(\lambda'_{1,2}) = 0$ . And for the critical wave number can be written as

$$(\mathbf{k}_c^n)^2 = \frac{d_h J_{11} + d_p J_{22}}{2d_p d_h}, \quad (\text{A10})$$

$J_{11}$  and  $J_{22}$  are the elements of the Matrix  $J$ .

Table II lists the eigenvalues of the Jacobian matrix (A9) and the critical wave number  $\mathbf{k}_c^n$ , from which one can see that our simulation outside the Turing instability regime when the  $f = 0.30$ .

The Maple program available on request.

- 
- [1] Janet W. Campbell. The university of new hampshire center of excellence for coastal ocean observation and analysis (semi-annual technical report: Na16oc2740). The Coastal Observing Center at UNH, 2005. The two satellite images were obtained from NASA's Ocean Color website: <http://oceancolor.gsfc.nasa.gov>, under the "image gallery" section.
- [2] Luis M. A. Bettencourt, Aric A. Hagberg, and Levi B. Larkey. Separating the wheat from the chaff: Practical anomaly detection schemes in ecological applications of distributed sensor networks. LA-UR-06-8235, 2007.
- [3] Edward R. Abraham and Melissa M. Bowen. Chaotic stirring by a mesoscale surface-ocean flow. *Chaos*, 12:373–381, 2002.
- [4] E. G. Durbin, R. G. Campbell, M. C. Casas, M. D. Ohman, B. Niehoff, J. Runge, and M. Wagner. Interannual variation in phytoplankton blooms and zooplankton productivity and abundance in the gulf of maine during winter. *Mar. Ecol.-Prog. Ser.*, 254:81–100, 2003.
- [5] C. L. May, J. R. Koseff, L. V. Lucas, J. E. Cloern, and D. H. Schoellhamer. Effects of spatial and temporal variability of turbidity on phytoplankton blooms. *Mar. Ecol.-Prog. Ser.*, 254:111–128, 2003.
- [6] Gregor F. Fussman, Stephen P. Ellner, Nelson G. Hairston, Laura E. Jones Jr., Kyle W. Shertzer, and Takehito Yoshida. *Population Dynamics and Laboratory Ecology*, chapter Ecological and Evolutionary Dynamics of Experimental Plankton Communities, page 221. Advances in ecological research; v.37. Elsevier Academic Press, Amsterdam; Oxford, 2005. Edited by R. A. Detharnais.
- [7] E.E. Popova, M.J.R. Fasham, A.V. Osipov, and V.A. Ryabchenko. Chaotic behaviour of an ocean ecosystem model under seasonal external forcing. *J. Plankton Res.*, 19:1495–1515, 1997.
- [8] Eckart Steffen, Horst Malchow, and Alexander B. Medvinsky. Effects of seasonal perturbations on a model plankton community. *Environ. Model. Assess.*, 2:43–48, 1997.
- [9] Horst Malchow. Spatial-temporal pattern formation in nonlinear non-equilibrium plankton dynamics. *Proc. R. Soc. Lond. B*, 251:103–109, 1993.
- [10] Roberto Benzi. Stochastic resonance: from climate to biology, 2007. arXiv.org:nlin/0702008.
- [11] H. Malchow, F. M. Hilker, and S. V. Petrovskii. Noise and productivity dependence of spatiotemporal pattern formation in a prey-predator system. *Discrete Cont. Dyn. Syst. B*, 4:705–711, 2004.
- [12] J. M. G. Vilar, R. V. Sole, and J. M. Rubi. On the origin of plankton patchiness. *Physica A*, 317:239–246, 2003.
- [13] Kenneth S. Johnson, David M. Karl, S. W. Chisholm, P. G. Falkowski, and J. J. Cullen. Is Ocean Fertilization Credible and Creditable? *Science*, 296:467–468, 2002.
- [14] Francesc Sagués, José M. Sancho, and Jordi García-Ojalvo. Spatiotemporal order out of noise. *Rev. Mod. Phys.*, 79:829, 2007.
- [15] Jordi Garca-Ojalvo and Jose M. Sancho. *Noise in spatially extended systems*. Springer, New York, 1999.
- [16] W. Horsthemke and R. Lefever. *Noise-induced transitions*. Springer series in synergetics; v.15. Springer-Verlag, Berlin; New York, 1984.
- [17] Luca Gammaitoni, Peter Hanggi, Peter Jung, and Fabio Marchesoni. Stochastic resonance. *Rev. Mod. Phys.*, 70:223, 1998.
- [18] Peter Jung and Gottfried Mayer-Kress. Spatiotemporal stochastic resonance in excitable media. *Phys. Rev. Lett.*, 74:2130–2133, 1995.
- [19] Luca Gammaitoni, Peter Hänggi, Peter Jung, and Fabio Marchesoni. Stochastic resonance. *Rev. Mod. Phys.*, 70:223–287, 1998.
- [20] Alexander Neiman, Lutz Schimansky-Geier, Ann Cornell-Bell, and Frank Moss. Noise-enhanced phase

- synchronization in excitable media. *Phys. Rev. Lett.*, 83:4896–4899, 1999.
- [21] Bambi Hu and Changsong Zhou. Phase synchronization in coupled nonidentical excitable systems and array-enhanced coherence resonance. *Phys. Rev. E*, 61:R1001–R1004, 2000.
- [22] Changsong Zhou, Jürgen Kurths, and Bambi Hu. Array-enhanced coherence resonance: Nontrivial effects of heterogeneity and spatial independence of noise. *Phys. Rev. Lett.*, 87:098101, 2001.
- [23] Changsong Zhou and Jürgen Kurths. Noise-sustained and controlled synchronization of stirred excitable media by external forcing. *New J. Phys.*, 7:18, 2005.
- [24] J. Buceta, M. Ibañes, J. M. Sancho, and Katja Lindenberg. Noise-driven mechanism for pattern formation. *Phys. Rev. E*, 67:021113, 2003.
- [25] Hongli Wang, Ke Zhang, and Qi Ouyang. Resonant-pattern formation induced by additive noise in periodically forced reaction-diffusion systems. *Phys. Rev. E*, 74:036210, 2006.
- [26] Miguel A. Santos and J. M. Sancho. Noise-induced fronts. *Phys. Rev. E*, 59:98, 1999.
- [27] L. Q. Zhou, X. Jia, and Q. Ouyang. Experimental and numerical studies of noise-induced coherent patterns in a subexcitable system. *Phys. Rev. Lett.*, 88:138301, 2002.
- [28] A. A. Zaikin and L. Schimansky-Geier. Spatial patterns induced by additive noise. *Phys. Rev. E*, 58:4355–4360, 1998.
- [29] S. S. Riaz, S. Dutta, S. Kar, and D. S. Ray. Pattern formation induced by additive noise: a moment-based analysis. *Eur. Phys. J. B*, 47:255–263, 2005.
- [30] F. Marchesoni, L. Gammaitoni, and A. R. Bulsara. Spatiotemporal stochastic resonance in a  $\varphi^4$  model of kink-antikink nucleation. *Phys. Rev. Lett.*, 76(15):2609–2612, 1996.
- [31] X. Sailer, D. Hennig, V. Beato, H. Engel, and L. Schimansky-Geier. Regular patterns in dichotomically driven activator-inhibitor dynamics. *Phys. Rev. E*, 73:056209, 2006.
- [32] B. Spagnolo, D. Valenti, and A. Fiasconaro. Noise in ecosystems: A short review. *Math. Biosci. Eng.*, 1:185–211, 2004.
- [33] Carl Zimmer. Complex Systems: Life After Chaos. *Science*, 284:83–86, 1999.
- [34] Ottar N. Bjornstad and Bryan T. Grenfell. Noisy Clockwork: Time Series Analysis of Population Fluctuations in Animals. *Science*, 293:638–643, 2001.
- [35] S. Ciuchi, F. de Pasquale, and B. Spagnolo. Self-regulation mechanism of an ecosystem in a non-gaussian fluctuation regime. *Phys. Rev. E*, 54:706–716, 1996.
- [36] José M. G. Vilar and Ricard V. Solé. Effects of noise in symmetric two-species competition. *Phys. Rev. Lett.*, 80:4099–4102, 1998.
- [37] Irene Giardina, Jean-Philippe Bouchaud, and Marc Mézard. Proliferation assisted transport in a random environment. *J. Phys. A: Math. Gen.*, 34:L245–L252, 2001.
- [38] B. Spagnolo and A. La Barbera. Role of the noise on the transient dynamics of an ecosystem of interacting species. *Physica A*, 315:114–124, 2002.
- [39] D. Valenti, A. Fiasconaro, and B. Spagnolo. Stochastic resonance and noise delayed extinction in a model of two competing species. *Physica A*, 331:477–486, 2004.
- [40] Mercedes Pascual. Computational ecology: From the complex to the simple and back. *Plos Comput. Biol.*, 1:e18, 2005.
- [41] Marten Scheffer. Fish and nutrients interplay determines algal biomass: a minimal model. *Oikos*, 62:271, 1991.
- [42] Alexander B. Medvinsky, Irene A. Tikhonova, Rubin R. Aliev, Bai-Lian Li, Zhen-Shan Lin, and Horst Malchow. Patchy environment as a factor of complex plankton dynamics. *Phys. Rev. E*, 64:021915, 2001.
- [43] Alexander B. Medvinsky, Sergei V. Petrovskii, Irene A. Tikhonova, Horst Malchow, and Bai-Lian Li. Spatiotemporal complexity of plankton and fish dynamics. *SIAM Review*, 44:311–370, 2002.
- [44] Horst Malchow. Spatio-temporal pattern formation in nonlinear nonequilibrium plankton dynamics. *Proc. R. Soc. London Ser. B*, 251:103–109, 1993.
- [45] Mercedes Pascual. Diffusion-induced chaos in a spatial predator-prey system. *Proc. R. Soc. Lond. B*, 251:1–7, 1993.
- [46] Kevin L. Kirk and John J. Gilbert. Variation in herbivore response to chemical defenses: Zooplankton foraging on toxic cyanobacteria. *Ecology*, 73:2208–2217, 1992.
- [47] J. E. Truscott and J. Brindley. Ocean plankton populations as excitable media. *Bull. Math. Biol.*, 56:981–998, 1992.
- [48] E J Buskey and D A Stockwell. *Toxic Phytoplankton Blooms in the Sea*, chapter effects of a persistent ‘brown-tide’ on zooplankton population in hte Laguna Madre of Southern Texas, pages 659–666. Elsevier, Amsterdam, 1993.
- [49] Sergei V. Petrovskii and Horst Malchow. Wave of chaos: New mechanism of pattern formation in spatio-temporal population dynamics. *Theor. Popul. Biol.*, 59:157–174, 2001.
- [50] In the physical world, the assumption that the fluctuations are fast in comparison with the relevant systems time scales may not always be true. To approximate such fluctuations by noise terms that are  $\delta$ -correlated would be inappropriate, and the result systems would produce inaccurate predictions. Here, we use the colored noise with an exponential time-correlated.
- [51] Marcus R. Garvie and Catalin Trenchea. Optimal control of a nutrient-phytoplankton-zooplankton-fish system. *SIAM J. Cont. and Opti.*, 46:775–791, 2007.
- [52] Quan-Xing Liu, Gui-Quan Sun, Bai-Lian Li, and Zhen Jin. Emergence of spatiotemporal chaos driven by far-field breakup of spiral waves in the plankton ecological systems. *arXiv:0704.0322*, 2007.
- [53] Björn Sandstede and Arnd Scheel. Period-doubling of spiral waves and defects. *SIAM J. Appl. Dynam. Syst.*, 6:494–547, 2007.
- [54] Sergei Petrovskii, Bai-Lian Li, and Horst Malchow. Transition to spatiotemporal chaos can resolve the paradox of enrichment. *Ecological Complexity*, 1:37–47, 2004.
- [55] W. G. Wilson. Resolving discrepancies between deterministic population models and individual-based simulations. *Am. Nat.*, 151:116–134, 1998.
- [56] This steady state loses stability in a Hopf bifurcation to oscillations in the zero-dimensional mode as the parameter  $f$  is decreased below a critical value  $f_H = 0.3397$ .
- [57] [www.iop.org](http://www.iop.org).
- [58] Fen-Ni Si, Quan-Xing Liu, Jin-Zhong Zhang, and Lu-Qun Zhou. Propagation of travelling waves in subexcitable systems driven by noise and periodic forcing. *Eur. Phys. J. B*, 60:Inpress, 2007. arXiv:0706.1917.
- [59] Valery Petrov, Qi Ouyang, and Harry L. Swinney. Res-

- onant pattern formation in a chemical system. *Nature*, 388:655–657, 1997.
- [60] Anna L. Lin, Aric Hagberg, Ehud Meron, and Harry L. Swinney. Resonance tongues and patterns in periodically forced reaction-diffusion systems. *Phys. Rev. E*, 69:066217, 2004.
- [61] J. M. T. Thompson and H. B. Stewart. *Nonlinear dynamics and chaos: geometrical methods for engineers and scientists*. Wiley, Chichester; New York, 1986.
- [62] Pierre Coulet and Kjartan Emilsson. Strong resonances of spatially distributed oscillators: a laboratory to study patterns and defects. *Physical D*, 61:119–131, 1992.
- [63] Zoltán Neufeld, Cristóbal López, Emilio Hernández-García, and Oreste Piro. Excitable media in open and closed chaotic flows. *Phys. Rev. E*, 66:066208, 2002.
- [64] Changsong Zhou, Jürgen Kurths, Zoltán Neufeld, and István Z. Kiss. Noise-sustained coherent oscillation of excitable media in a chaotic flow. *Phys. Rev. Lett.*, 91:150601, 2003.
- [65] Emilio Hernandez-Garcia and Cristobal Lopez. Sustained plankton blooms under open chaotic flows. *Ecological Complexity*, 1:253–259, 2004.
- [66] Z. Neufeld, P. H. Haynes, V. Garçon, and J. Sudre. Ocean fertilization experiments may initiate a large scale phytoplankton bloom. *Geop. Res. Lett.*, 29:1534, 2002.
- [67] Emilio Hernandez-Garcia, Cristobal Lopez, and Zoltan Neufeld. Small-scale structure of nonlinearly interacting species advected by chaotic flows. *Chaos*, 12:470, 2002.
- [68] A. Tzella and P. H. Haynes. Small-scale spatial structure in plankton distributions. *Biogeosciences*, 4:173–179, 2007.
- [69] R. Reigada, R. M. Hillary, M. A. Bees, J. M. Sancho, and F. Sagues. Plankton blooms induced by turbulent flows. *Proc. R. Soc. Lond. B*, 270:875–880, 2003.
- [70] A. J. Koch and H. Meinhardt. Biological pattern formation: from basic mechanisms to complex structures. *Rev. Mod. Phys.*, 66:1481–1507, 1994.